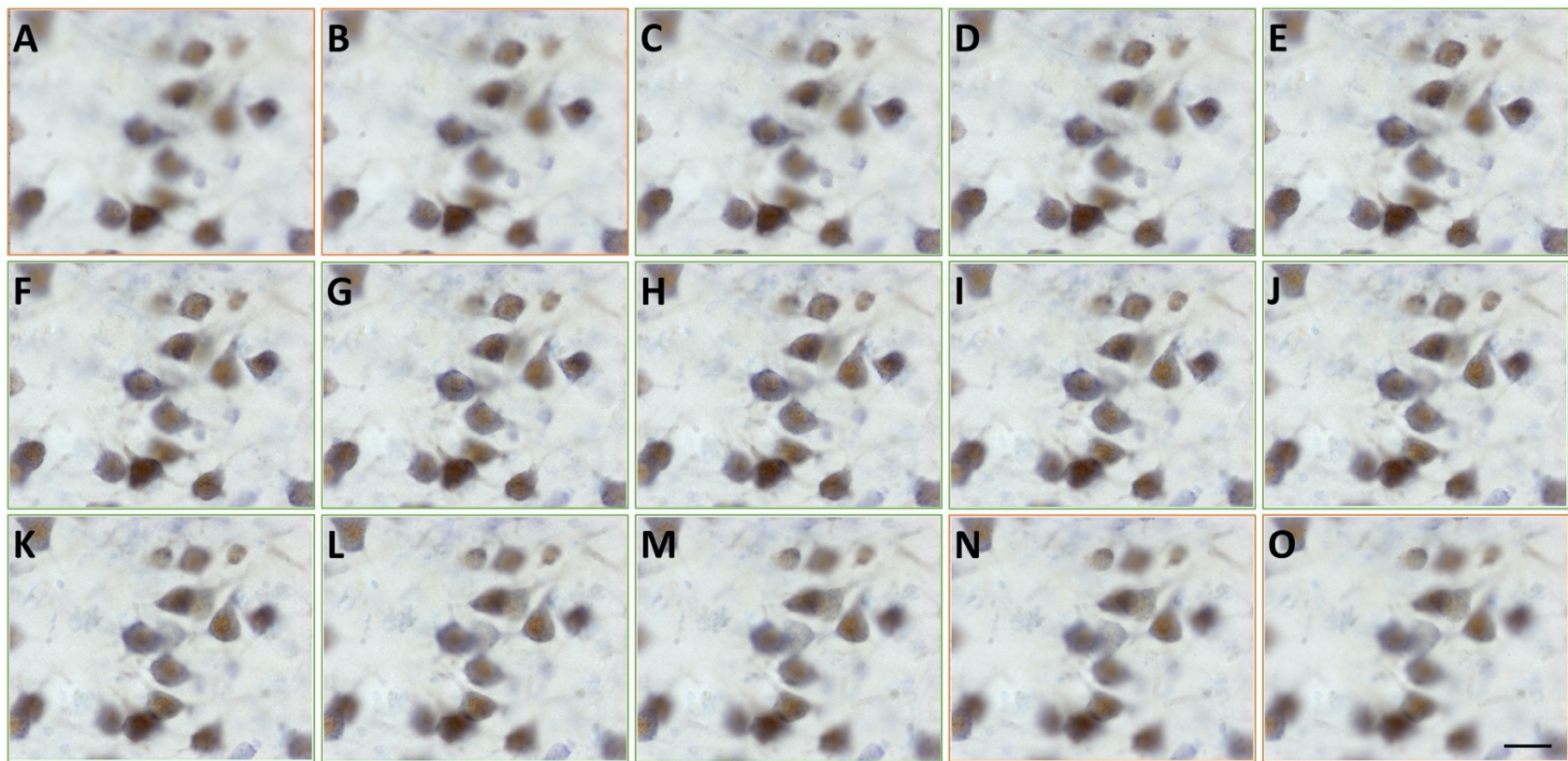
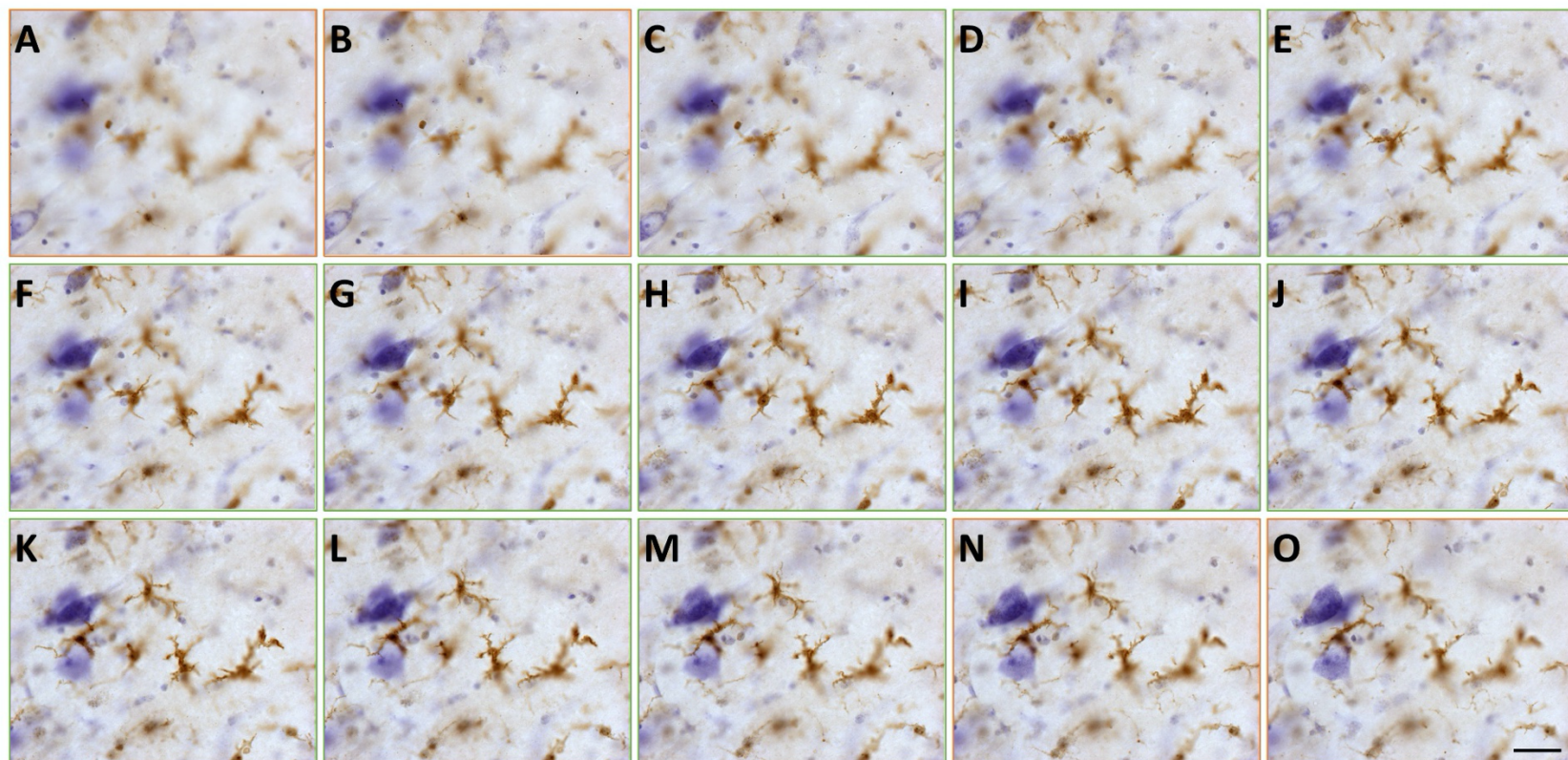


Supplementary Material

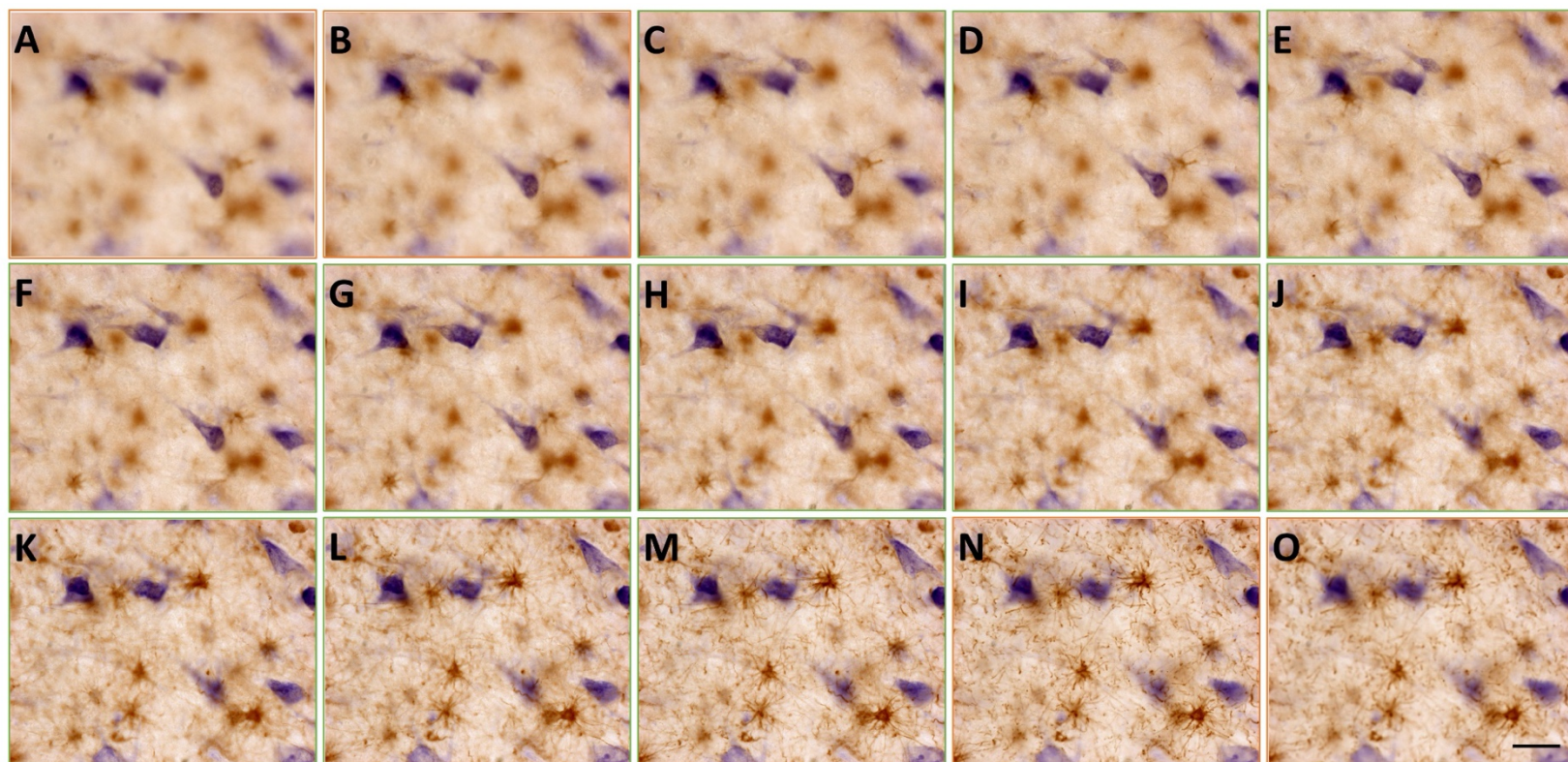
The Human Hippocampus in Parkinson's Disease: An Integrative Stereological and Proteomic Study



Supplementary Figure 2. Demonstration of NeuN-stained penetration in a section used for Z-axis. Images of NeuN-stained penetration in the human hippocampus section used for Z axis analysis (A-O). Orange (A, B, N, O) and green contours (C-M) represent the guard zones ($\pm 2 \mu\text{m}$) and the height disector ($11 \mu\text{m}$), respectively. Presented are evenly spaced focal planes through a section for z axis with intervals of $1 \mu\text{m}$ from top (A) to bottom (O). Scale bar $25 \mu\text{m}$.



Supplementary Figure 3. Demonstration of Iba1-stained penetration in a section used for Z-axis. Images of Iba-1-stained penetration in the human hippocampus section used for Z axis analysis (A-O). Orange (A, B, N, O) and green contours (C-M) represent the guard zones ($\pm 2 \mu\text{m}$) and the height dissector ($11 \mu\text{m}$), respectively. Presented are evenly spaced focal planes through a section for z axis with intervals of $1 \mu\text{m}$ from top (A) to bottom (O). Scale bar $25 \mu\text{m}$.



Supplementary Figure 4. Demonstration of GFAP-stained penetration in a section used for Z-axis. Images of GFAP-stained penetration in the human hippocampus section used for Z axis analysis (A-O). Orange (A, B, N, O) and green contours (C-M) represent the guard zones ($\pm 2 \mu\text{m}$) and the height disector (11 μm), respectively. Presented are evenly spaced focal planes through a section for z axis with intervals of 1 μm from top (A) to bottom (O). Scale bar 25 μm .

Supplementary Table 1. Area fraction occupied by α -syn.

Supplementary Table 1a. Area fraction occupied by α -syn in DG.

Case	Number of Sections	Section Cut Thickness (μm)	Section Evaluation Interval	Counting Frame Area (XY) (μm^2)	Sampling Grid Area (XY) (μm^2)	Grid Spacing (μm)	Number of Sampling Sites	Total Markers Counted	Area Sampling Fraction	Area Fraction	Estimated area (μm^2)	Gundersen error m=1
1	4	50	13	90,000	640,000	20	98	93	0.14	0.0053	264,533.0	0.05
2	4	50	13	90,000	160,000	20	139	51	0.56	0.0022	36,266.7	0.05
5	3	50	13	90,000	160,000	20	99	44	0.56	0.0034	31,288.9	0.07
6	4	50	13	90,000	1,000,000	20	66	55	0.09	0.0056	244,444.0	0.06
7	4	50	13	90,000	2,250,000	20	35	32	0.04	0.0065	320,000.0	0.08
8	4	50	13	90,000	160,000	20	262	25	0.56	0.0006	17,777.8	0.09
11	4	50	13	90,000	640,000	20	60	45	0.14	0.0042	128,000.0	0.06
13	4	50	13	90,000	160,000	20	210	36	0.56	0.0011	25,600.0	0.08
15	4	50	13	90,000	1,000,000	20	42	50	0.09	0.0081	222,222.0	0.05

Supplementary Table 1b. Area fraction occupied by α -syn in CA3.

Case	Number of Sections	Section Cut Thickness (μm)	Section Evaluation Interval	Counting Frame Area (XY) (μm^2)	Sampling Grid Area (XY) (μm^2)	Grid Spacing (μm)	Number of Sampling Sites	Total Markers Counted	Area Sampling Fraction	Area Fraction	Estimated area (μm^2)	Gundersen error m=1
6	4	50	13	90,000	1,000,000	30	42	90	0.09	0.0298	900,000.0	0.05
7	4	50	13	90,000	1,000,000	20	50	363	0.09	0.0425	1,613,330.0	0.04
8	4	50	13	90,000	160,000	20	253	80	0.56	0.0018	56,888.9	0.03
11	4	50	13	90,000	1,000,000	20	13	31	0.09	0.0143	137,778.0	0.06
13	4	50	13	90,000	160,000	20	67	14	0.56	0.0014	9,955.6	0.11
15	4	50	13	90,000	360,000	30	35	50	0.25	0.0277	180,000.0	0.05

Supplementary Table 1c. Area fraction occupied by α -syn in CA2.

Case	Number of Sections	Section Cut Thickness (μm)	Section Evaluation Interval	Counting Frame Area (XY) (μm^2)	Sampling Grid Area (XY) (μm^2)	Grid Spacing (μm)	Number of Sampling Sites	Total Markers Counted	Area Sampling Fraction	Area Fraction	Estimated area (μm^2)	Gundersen error m=1
1	4	50	13	90,000	640,000	40	53	36	0.14	0.0158	409,600.0	0.08
2	4	50	13	90,000	160,000	40	82	37	0.56	0.0102	105,244.0	0.07
5	3	50	13	90,000	160,000	20	51	19	0.56	0.0028	13,511.1	0.09
6	4	50	13	90,000	1,000,000	40	32	108	0.09	0.0824	1,920,000.0	0.06
7	4	50	13	90,000	1,000,000	40	37	113	0.09	0.0716	2,008,890.0	0.05
8	4	50	13	90,000	360,000	40	82	20	0.25	0.0063	128,000.0	0.10
11	4	50	13	90,000	360,000	40	47	68	0.25	0.0405	435,200.0	0.05
13	4	50	13	90,000	160,000	20	98	64	0.56	0.0048	45,511.1	0.05
15	4	50	13	90,000	360,000	40	48	205	0.25	0.1310	1,312,000.0	0.02

Supplementary Table 1d. Area fraction occupied by α -syn in CA1.

Case	Number of Sections	Section Cut Thickness (μm)	Section Evaluation Interval	Counting Frame Area (XY) (μm^2)	Sampling Grid Area (XY) (μm^2)	Grid Spacing (μm)	Number of Sampling Sites	Total Markers Counted	Area Sampling Fraction	Area Fraction	Estimated area (μm^2)	Gundersen error m=1
1	4	50	13	90,000	1,440,000	20	150	196	0.06	0.0072	1,254,400.0	0.04
2	4	50	13	90,000	16,000,000	20	15	37	0.01	0.0125	2,631,110.0	0.08
5	3	50	13	90,000	640,000	20	113	50	0.14	0.0028	142,222.0	0.07
6	4	50	13	90,000	1,000,000	20	60	78	0.09	0.0077	346,667.0	0.04
7	4	50	13	90,000	1,000,000	20	65	69	0.09	0.0064	306,667.0	0.05
8	4	50	13	90,000	160,000	20	349	62	0.56	0.0010	44,088.9	0.05
11	4	50	13	90,000	4,000,000	20	15	41	0.02	0.0174	728,889.0	0.07
13	4	50	13	90,000	160,000	20	438	72	0.56	0.0010	51,200.0	0.05
15	4	50	13	90,000	4,000,000	20	14	49	0.02	0.0179	871,111.0	0.08

Supplementary Table 2. Volume data.

Supplementary Table 2a. Estimated HP volume.

Case	Number of Sections	Section Cut Thickness (μm)	Section Evaluation Interval	Grid Size (μm)	Count	Estimated Area (mm^2)	Volume Corrected for Over Projection (mm^3)	Gundersen error m=1
1	4	50	13	250	5,408	338.00	214.86	0.03
2	4	50	13	250	5,621	351.31	223.41	0.02
3	4	50	13	250	3,283	205.19	130.61	0.02
4	4	50	13	250	5,924	370.25	235.90	0.02
5	4	50	13	250	5,214	325.87	207.54	0.02
6	4	50	13	250	3,218	201.12	127.89	0.02
7	4	50	13	250	3,611	225.69	143.26	0.02
8	4	50	13	250	2,769	173.06	110.10	0.02
9	4	50	13	250	3,822	238.87	152.03	0.02
10	4	50	13	250	3,845	240.31	153.10	0.02
11	5	50	13	250	3,505	219.06	140.04	0.02
12	5	50	13	250	4,427	276.69	176.78	0.02
13	5	50	13	250	3,434	214.62	137.15	0.02
14	5	50	13	250	3,600	225.00	143.73	0.02
15	5	50	13	250	3,077	192.31	123.03	0.02
22	4	50	13	250	3,848	240.50	153.25	0.02
23	4	50	13	250	3,612	225.75	143.80	0.02
24	4	50	13	250	4,473	279.56	177.92	0.03
25	4	50	13	250	4,050	253.12	161.12	0.02
26	4	50	13	250	5,457	341.06	216.92	0.02
27	4	50	13	250	4,195	262.19	164.13	0.04
28	4	50	13	250	3,350	209.37	133.18	0.02
29	4	50	13	250	6,288	393.00	250.39	0.02
30	4	50	13	250	3,408	213.00	135.72	0.02
31	4	50	13	250	3,769	235.56	149.50	0.02
32	5	50	13	250	2,787	174.19	111.25	0.02
33	5	50	13	250	3,619	226.19	144.70	0.02
34	5	50	13	250	3,087	192.94	123.37	0.02
35	5	50	13	250	3,930	245.62	157.08	0.02
36	5	50	13	250	2,978	186.12	119.03	0.02

*Gray shade shows PD cases.

Supplementary Table 2b. Estimated DG volume.

Case	Number of Sections	Section Cut Thickness (μm)	Section Evaluation Interval	Grid Size (μm)	Count	Estimated Area (mm^2)	Volume Corrected for Over Projection (mm^3)	Gundersen error m=1
1	4	50	13	250	917	57.31	36.14	0.05
2	2	50	13	250	180	11.25	6.90	0.07
3	4	50	13	250	1,060	66.25	41.82	0.03
4	4	50	13	250	1,272	79.50	50.29	0.03
5	5	50	13	250	497	31.06	19.44	0.04
6	4	50	13	250	772	48.25	30.37	0.04
7	4	50	13	250	920	57.50	36.55	0.02
8	4	50	13	250	750	46.87	29.53	0.04
9	4	50	13	250	860	53.75	34.07	0.03
10	4	50	13	250	904	56.50	35.80	0.03
11	5	50	13	250	1,027	64.19	40.95	0.02
12	5	50	13	250	1,292	80.75	51.58	0.01
13	5	50	13	250	824	51.50	32.93	0.02
14	5	50	13	250	949	59.31	37.81	0.02
15	5	50	13	250	838	52.37	33.47	0.02
21	4	50	13	250	731	45.69	28.82	0.03
22	2	50	13	250	164	10.25	6.35	0.05
23	3	50	13	250	877	54.81	34.07	0.05
24	4	50	13	250	745	46.56	29.21	0.05
25	3	50	13	250	936	58.50	36.42	0.04
26	4	50	13	250	1,402	87.62	55.37	0.03
27	4	50	13	250	805	50.31	31.72	0.03
28	4	50	13	250	2,077	129.81	82.39	0.02
29	4	50	13	250	1,146	71.62	45.32	0.03
30	4	50	13	250	1,715	107.19	68.17	0.02
31	5	50	13	250	833	52.06	33.27	0.02
32	5	50	13	250	1,031	64.44	41.10	0.02
33	5	50	13	250	1,032	64.50	41.22	0.02
34	5	50	13	250	1,134	70.87	45.33	0.02
35	5	50	13	250	827	51.69	33.02	0.02

*Gray shade shows PD cases.

Supplementary Table 2e. Estimated CA1 volume.

Case	Number of Sections	Section Cut Thickness (μm)	Section Evaluation Interval	Grid Size (μm)	Count	Estimated Area (mm^2)	Volume Corrected for Over Projection (mm^3)	Gundersen error m=1
1	4	50	13	250	3,916	244.75	155.87	0.02
2	4	50	13	250	5,232	327.00	208.17	0.02
3	4	50	13	250	2,009	125.56	79.71	0.02
4	4	50	13	250	4,251	265.69	169.11	0.02
5	4	50	13	250	4,464	279.00	177.49	0.02
6	4	50	13	250	1,118	69.87	44.48	0.02
7	4	50	13	250	1,312	82.00	52.22	0.02
8	4	50	13	250	902	56.37	35.88	0.02
9	4	50	13	250	1,433	89.56	57.05	0.02
10	4	50	13	250	1,884	117.75	74.92	0.02
11	5	50	13	250	1,768	110.50	70.61	0.02
12	5	50	13	250	2,417	151.06	96.19	0.02
13	5	50	13	250	2,124	132.75	84.80	0.02
14	5	50	13	250	2,141	133.81	85.49	0.02
15	5	50	13	250	1,852	115.75	73.97	0.02
21	4	50	13	250	2,843	177.69	112.83	0.02
22	4	50	13	250	3,368	210.50	133.91	0.02
23	4	50	13	250	3,099	193.69	122.29	0.03
24	4	50	13	250	2,785	174.06	110.70	0.02
25	4	50	13	250	4,033	252.06	159.83	0.02
26	4	50	13	250	1,162	72.62	45.37	0.04
27	4	50	13	250	1,198	74.87	47.66	0.02
28	4	50	13	250	2,139	133.69	85.10	0.02
29	4	50	13	250	1,334	83.37	52.97	0.03
30	4	50	13	250	1,499	93.69	59.65	0.02
31	5	50	13	250	1,502	93.87	59.90	0.01
32	5	50	13	250	1,911	119.44	76.36	0.02
33	5	50	13	250	1,585	99.06	63.29	0.02
34	5	50	13	250	2,147	134.19	85.80	0.02
35	5	50	13	250	1,702	106.37	68.00	0.02

*Gray shade shows PD cases.

Supplementary Table 3b. Estimated CA3 neuron number and density.

Case	Number of Sections	Section Cut Thickness (μm)	Section Evaluation Interval	Disector Height (Z) (μm)	Guard Zone Distance (μm)	Mean Measured Section Thickness (μm)	Counting	Sampling Grid Area (XY) (μm ²)	Number of Sampling Sites	Total Markers Counted	Estimated Popu lation using Mean Section Thickness	Measured Volume (mm ³)	Gundersen error m=1	Density (cell/mm ³)
							Frame Area (XY) (μm ²)							
6	4	50	13	11	2	15.82	2,500	202,500	162	159	240,719.25	20.22	0.08	11,903.12
7	4	50	13	11	2	14.45	2,500	202,500	190	169	233,780.53	24.20	0.08	9,659.67
8	4	50	13	11	2	13.67	2,500	250,000	154	150	242,319.19	23.78	0.09	10,189.14
9	4	50	13	11	2	13.47	2,500	250,000	184	203	323,265.16	28.47	0.07	11,355.07
10	3	50	13	11	2	13.64	2,500	160,000	157	128	192,954.34	22.80	0.09	8,464.47
11	5	50	13	11	2	16.49	2,500	22,500	866	638	111,886.55	11.70	0.05	9,562.95
12	5	50	13	11	2	15.64	2,500	22,500	732	634	105,472.50	9.54	0.04	11,054.31
13	5	50	13	11	2	16.18	2,500	22,500	582	342	58,859.34	7.70	0.06	7,644.07
14	5	50	13	11	2	15.30	2,500	22,500	487	246	40,036.55	6.58	0.07	6,079.93
15	5	50	13	11	2	14.93	2,500	22,500	533	374	59,385.89	7.10	0.06	8,364.21
26	4	50	13	11	2	14.25	2,500	202,500	189	184	250,980.34	23.48	0.08	10,687.02
27	4	50	13	11	2	15.46	2,500	202,500	174	159	235,318.45	21.66	0.09	10,862.09
28	4	50	13	11	2	14.68	2,500	202,500	208	202	283,927.66	25.80	0.09	11,004.73
29	2	50	13	11	2	14.67	2,500	90,000	163	175	109,220.39	8.89	0.09	12,285.08
30	4	50	13	11	2	14.05	2,500	202,500	121	95	127,727.96	15.61	0.10	8,183.91
31	5	50	13	11	2	17.25	2,500	22,500	445	361	66,218.80	5.90	0.06	11,223.52
32	5	50	13	11	2	16.23	2,500	22,500	573	417	71,982.09	7.70	0.06	9,348.32
33	5	50	13	11	2	14.78	2,500	22,500	600	287	45,112.04	8.10	0.06	5,569.39
34	5	50	13	11	2	13.86	2,500	90,000	215	176	103,783.93	11.80	0.08	8,793.98
35	5	50	13	11	2	13.70	2,500	90,000	175	164	95,575.64	9.43	0.08	10,131.88

*Gray shade shows PD cases.

Supplementary Table 4b. Estimated CA3 microglia number and density.

Case	Number of Sections	Section Cut Thickness (μm)	Section Evaluation Interval	Disector Height (Z) (μm)	Guard Zone Distance (μm)	Mean Measured Section Thickness (μm)	Counting Frame Area (XY) (μm ²)	Sampling Grid Area (XY) (μm ²)	Number of Sampling Sites	Total Markers Counted	Estimated Population using Mean Section Thickness		Measured Volume (mm ³)	Gundersen error m=1	Density (cell/mm ³)
6	4	50	13	11	2	14.98	2,500	250,000	137	288	509,774.03	20.41	0.06	24,974.97	
7	4	50	13	11	2	13.91	2,500	250,000	172	252	414,150.88	27.33	0.07	15,154.60	
8	4	50	13	11	2	13.59	2,500	250,000	147	208	334,106.06	23.91	0.07	13,971.73	
9	4	50	13	11	2	13.47	2,500	422,500	106	125	336,350.75	27.31	0.09	12,316.84	
10	3	50	13	11	2	14.51	2,500	250,000	65	124	212,703.53	9.99	0.09	21,288.81	
11	5	50	13	11	2	15.42	2,500	90,000	163	253	165,986.66	8.70	0.07	19,081.71	
12	5	50	13	11	2	15.76	2,500	22,500	835	420	70,410.02	11.22	0.05	6,272.89	
13	5	50	13	11	2	15.02	2,500	90,000	110	128	81,785.47	5.65	0.09	14,477.10	
14	5	50	13	11	2	14.77	2,500	90,000	104	142	89,248.59	5.78	0.09	15,444.22	
15	5	50	13	11	2	15.01	2,500	90,000	91	160	102,144.06	4.63	0.08	22,043.31	
26	4	50	13	11	2	14.02	2,500	250,000	129	235	389,302.69	20.44	0.08	19,042.30	
27	4	50	13	11	2	15.10	2,500	250,000	150	157	280,124.06	21.99	0.09	12,737.72	
28	4	50	13	11	2	14.58	2,500	250,000	165	132	227,376.94	25.93	0.10	8,767.25	
29	2	50	13	11	2	13.49	2,500	160,000	90	157	480,513.44	26.96	0.09	17,821.81	
30	3	50	13	11	2	13.69	2,500	202,500	93	118	154,601.11	11.03	0.10	14,017.56	
31	5	50	13	11	2	16.29	2,500	40,000	249	105	28,250.94	5.78	0.10	4,889.25	
32	5	50	13	11	2	15.76	2,500	90,000	157	261	175,008.58	8.60	0.06	20,358.66	
33	5	50	13	11	2	14.72	2,500	90,000	172	203	127,126.59	9.12	0.07	13,931.59	
34	5	50	13	11	2	15.10	2,500	90,000	199	255	163,836.31	10.73	0.07	15,270.56	
35	5	50	13	11	2	14.23	2,500	40,000	249	105	28,250.94	5.79	0.10	4,889.25	

*Gray shade shows PD cases.

Supplementary Table 6. Statistical data.

		Volume		NeuN Density		Iba-1 Density		GFAP Density	
		U/tdf	p	U/tdf	p	U/tdf	p	U/tdf	p
HP	R	U=7000	0.3095	U=7.000	0.5238	U=6.000	0.4127	t ₈ =1.043	0.3273
	I	t ₈ =1.266	0.2412	t ₈ =0.1251	0.9035	t ₈ =1.121	0.2948	t ₈ =0.4135	0.6901
	C	t ₈ =1.060	0.3201	t ₈ =0.1251	0.9035	t ₈ =0.4139	0.6898	t ₈ =0.9657	0.3625
	T	U=110.0	0.9237	t ₂₇ =0.4161	0.6806	t ₂₇ =0.1899	0.6898	t ₂₈ =0.09980	0.9212
DG	R	U=9000	0.5317	U=4.000	0.1905	U=5.000	0.2857	t ₈ =1.517	0.1677
	I	t _{4,208} =2.619	0.0559	t ₈ =1.366	0.2090	t ₈ =1.671	0.1332	t ₈ =1.073	0.3144
	C	t ₈ =0.1344	0.8964	t ₈ =0.2112	0.8380	t ₈ =0.4210	0.6848	t ₈ =0.2052	0.8425
	T	t ₂₈ =1.200	0.2403	t ₂₇ =1.379	0.1792	t ₂₇ =0.08727	0.9311	t ₂₈ =0.4883	0.6291
CA3	I	t ₈ =0.6203	0.5523	t ₈ =0.6203	0.5523	t ₈ =1.013	0.3406	t ₈ =0.2091	0.8396
	C	t ₈ =0.5296	0.6108	t ₈ =0.3710	0.7202	t ₈ =0.4321	0.6771	t ₈ =1.097	0.3045
	T	t ₁₈ =0.8987	0.3807	t ₁₈ =0.4558	0.6540	t ₁₈ =1.025	0.3191	t ₁₈ =0.5176	0.6110
CA2	R	t ₈ =0.4264	0.6810	U=6.000	0.4127	U=9.00	0.8730	U=8.000	0.4127
	I	t _{4,488} =2.045	0.1027	t ₈ =1.579	0.1529	t ₈ =1.071	0.3153	t ₈ =0.1732	0.8666
	C	t ₈ =0.07337	0.9433	t ₈ =0.1418	0.8907	t ₈ =0.8902	0.3994	t ₈ =1.200	0.2644
	T	t _{20,18} =1.260	0.2219	t ₂₇ =0.1958	0.8462	t ₂₇ =0.7308	0.4712	t ₂₈ =0.06758	0.9466
CA1	R	t ₈ =1.300	0.2298	t ₈ =0.3107	0.7640	U=8.000	0.7143	t ₈ =0.7513	0.4740
	I	t ₈ =0.5387	0.6047	t ₈ =0.7816	0.4569	t ₈ =1.798	0.1099	t ₈ =1.123	0.2942
	C	t ₈ =1.767	0.1153	U=12.00	0.9444	t ₈ =1.129	0.2917	t ₈ =1.287	0.2340
	T	U=105.0	0.7654	t ₂₈ =0.7877	0.4375	t ₂₇ =0.2354	0.2354	U=104.0	0.7346

C, caudal; CA, *Cornu ammonis*; DG, dentate gyrus; HP, hippocampus; I, intermediate; R, rostral; T, total

Supplementary Table 7. Systematic searches.

Three **systematic searches** were carried out with the following objectives:

Reviewing the existing literature that analyzed Lewy pathology in at least CA2 of the human hippocampus in PD.

The keywords "human AND hippocampus AND Lewy bodies AND Lewy neurites" were searched in PubMed on May 27, 2020. The search was filtered to the human species, other filters such as article type, text availability or the date of publication. 370 articles were listed as a result of the search. For a first filtering, it was taken into account that the title of the article had a clear relationship with the objective of the search, reducing the articles to 9. After reading the content of the 9 articles, 4 final articles were selected because they had all the information collected in the following table. This reading allowed access to specific citations from 5 other articles included in the final selection (Supplementary Table 7a).

Reviewing all the published articles on MRI and morphometry based on voxel that studied the volumetric changes of the human hippocampus of patients with PD, PDMIC or PDD.

The search was carried out on March 18, 2020. PubMed was used to search for the keywords "Human hippocampal AND Parkinson's disease AND magnetic resonance". Filters such as article type, text availability, publication date or species were not taken into account. 162 items were indicated as result of the search. For a first filtering it was taken into account that the title of the article had a clear relationship with the objective of the search. For those articles, whose title did not allow making a decision, the information in the summary was used. Finally, 40 articles were selected and classified depending on the groups of comparation and results (Supplementary Table 7b).

Reviewing all the published articles on MRI that studied the volumetric changes of the subfields of the human hippocampus of patients with PD, PDMIC or PDD.

The search was carried out on May 14, 2020. PubMed was used to search for the keywords "Human AND hippocampal subfields AND Parkinson's disease AND MRI" filtering by Human species. Other filters such as article type, text availability, or publication date were not taken into account. 9 items were indicated as a result of the search and 3 of them were discarded for studying other parameters, such as connectivity, instead of volume change; analyzing the changes in the volume of the hippocampal subfields produced by other variables than PD and not including CA2 measures, a field of special interest for our study (Supplementary Table 7c).

Supplementary Table 7a. Studies that analyzed Lewy pathology in human hippocampal subfields in PD

REFERENCE*	N	ANTIBODY	HP ZONE	AREA	QUANTIFICATION	
(Dickson et al 1994)	13PD	Ubiquitin (UltraClone, Ltd., Isle of Wight, UK)	Full length	CA2-3	Clinical signs compatible with PD	Semiquantitative
(Kim et al 1995)	2PD	Ubiquitin (East Acres Biologicals, Southbridge, MA)	Full length	CA2-3	Not specified	Semiquantitative
(Churchyard & Lees 1997)	10PD 7PDMID 10PD	Ubiquitin (Dako, Glostrup, Denmark)	HP at the level of <i>Cornu Ammonis</i> , and through the anterior cingulate gyrus at the level of the anterior frontal lobe.	CA1, CA2, CA3 and CA4	H&Y 3.6±0.3 H&Y 3.8±0.3 H&Y 4.0±0.3	Qualitatively
(Mattila et al 1999)	45PD	Ubiquitin (Dako, Glostrup, Denmark)	Full length	CA2-3	Not specified	Semiquantitative
(Harding & Halliday 2001)	25PD 16PDD	Ubiquitin (Dako, Glostrup, Denmark) α-syn (Zymed Laboratories, San Francisco, Calif)	HP at the level of the lateral geniculate nucleus	CA2	H&Y 2–3 and H&Y 4–5	Semiquantitative
(Braak et al 2003)	41PD	α-syn generated by W.P. Gai (Flinders Medical Centre, Australia)	Full length	CA2	PD stage 1-6	Semiquantitative
(Armstrong et al 2014)	15PDD	Ubiquitin (Dako, Glostrup, Denmark) α-syn-P (Wako Chemicals USA Inc., Richmond, VA)	Full length	CA1, CA2, CA3, CA4, DGm and DGg	Braak 5 and 6	Quantitative
(Flores-Cuadrado et al 2016)	3 PD	α-syn (Novocastra, Newcastle, UK)	Bregma 29-31 and 34-37	CA1, CA2, CA3 and DG	Braak 3, 4 and 5	Unbiased semiautomatic quantification

*See supplementary references. CA, Cornu ammonis; DG, dentate gyrus; DGm, molecular layer of dentate gyrus; DGg, granule layer of dentate gyrus; NPD, non Parkinson's disease; PD, Parkinson's disease; PDD, Parkinson's disease with dementia; PDMCI, Parkinson's disease with mild cognitive impairment.

Supplementary Table 7b. MRI studies about volume changes produced on human hippocampus in PD with and without dementia

	DECREASE VOLUME*	INCREASE VOLUME*	NO CHANGE VOLUME*
PD vs NPD	(Laakso et al 1996)	(Nyberg et al 2015)	(Burton et al 2004)
	(Camiccioli et al 2003)	(Zeng et al 2017)	(Nagano-Saito et al 2005)
	(Brück et al 2004)		(Junqué et al 2005)
	(Summerfield et al 2005)		(Apostolova et al 2010)
	(Aarsland 2006)		(Messina et al 2011)
	(Bouchard et al 2008)		(Melzer et al 2012)
	(Jokinen et al 2009)		(Carlesimo et al 2012)
	(Goldman et al 2012)		(Rektorova et al 2014)
	(Lee et al 2013)		(Chen et al 2015)
	(Zhang et al 2014)		(Yao et al 2016)
	(Lee et al 2014)		(Lenka et al 2018)
	(Noh et al 2014)		(Kamps et al 2018)
	(Cohn et al 2016)		
PDMCI vs NPD	(Radzunas et al 2018)		
	(Vasconcellos et al 2018)		
	(Melzer et al 2012)		(Apostolova et al 2010)
PDD vs NPD	(Noh et al 2014)		(Rektorova et al 2014)
	(Chen et al 2015)		(Kunst et al 2019)
	(Laakso et al 1996)		(Apostolova et al 2010)
	(Camiccioli et al 2003)		
	(Burton et al 2004)		
	(Nagano-Saito et al 2005)		
	(Summerfield et al 2005)		
	(Bouchard et al 2008)		
	(Junqué et al 2005)		
	(Jokinen et al 2010)		
	(Melzer et al 2012)		
	(Goldman et al 2012)		
	(Lee et al 2013)		
PDMCI vs PD	(Rektorova et al 2014)		
	(Novellino et al 2018)		
	(Kunst et al 2019)		
PDD vs PD	(Kandiah et al 2014)		
	(Noh et al 2014)		
	(Schneider et al 2017)		
PDD vs PDMCI	(Bouchard et al 2008)		(Cwc et al 2005)
	(Aybek et al 2009)		
	(Lee et al 2013)		
	(Kandiah et al 2014)		
	(Gee et al 2017)		
	(Low et al 2019)		
	(Mihaescu et al 2019)		
PDD vs PDMCI	(Chung et al 2017)		

*See supplementary references. NPD, non Parkinson's disease; PD, Parkinson's disease; PDD, Parkinson's disease with dementia; PDMCI, Parkinson's disease with mild cognitive impairment.

Supplementary Table 7c. MRI studies about volume changes produced on human hippocampus fields in PD with and without dementia.

REFERENCE*	N	AREA	RESULT
(Pereira et al 2013)	18 PD	F, PrS, S, CA1, CA2-3, CA4-DG and	Atrophy of CA2-3 and CA4-DG in PD compare to NPD
	18 PD with hallucinations	HPf	Atrophy of CA2-3, CA4-DG and S in PD with hallucinations compare to NPD
	18 NPD		
(Foo et al 2016)	11 PDMCI	F, alv, ml, PrS, PaS, S, CA1, CA2-3,	Atrophy of F(l), CA1(r) and HATA(r) in PDMCI compare to PD
	54 PD that convert to:	CA4, DGg, HPf, HPt and HATA	Basal atrophy of PaS(l), DGg, CA4(r) and HATA(l) in PDMCI-converters compare to PD-stables
	42 PD-stables	-	Atrophy of CA2-3(r) in PDMCI-converters compare to PD-stables
(Lenka et al 2018)	12 PDMCI converters	-	
	51PD	F, ml, PrS, PaS, S, CA1, CA2-3, CA4,	No differences between PD and NPD
	42PD with psychosis	DGg, HPf, HPt and HATA	Atrophy of ml, DGg, S(l), HPt(l), CA2-3(r), CA4(r) and HATA(r) and higher volume of HPf in PD with psychosis compare to NPD
(Novellino et al 2018)	48NPD		
	22AD	F, PrS, S, CA1, CA2-3, CA4-DG and	Atrophy of PrS(l) and CA2-3 in PDD compare to NPD
	18PDD	HPf	Atrophy of CA2-3, CA4-DG, PrS, S, F, in AD compare to NPD
(Low et al 2019)	17NPD		
	73PD that convert to:	F, ml, PrS, PaS, S, CA1, CA2-3, CA4,	Basal atrophy of CA1, S and PrS in PDD-converters compare to PD-stables
	62PD-stables	DGg, HPf, HPt and HATA	Atrophy of PaS, PrS and F in PDD-converters compare to PD-stables
(Wang et al 2019)	11PDD-converters		
	26PDMCI	alv, ml, PrS, PaS, S, CA1, CA2-3,	High volume of HPf in PDMCI compare to NPD
	30NPD	CA4, DGg, HPf, HPt, and HATA	Atrophy of ml, PrS(r), PaS(r), S(r), CA2-3(l), CA1(r), HATA in MSAMCI compare to NPD
	30MSAMCI		Atrophy of ml, PrS, PaS(r), CA2-3(l), CA1, HPt, HATA(r) in MSAMCI compare to PDMCI

*See supplementary references. AD, Alzheimer's disease; alv, alveus; CA, *Cornu ammonis*; DG, dentate gyrus; DGg, granule layer of dentate gyrus; F, fimbria; HATA, hippocampus-amygdala-transition; HPf, hippocampus fissure; HPt, hippocampus tail; (l), left; ml, molecular layer; MSAMCI, multiple system atrophy with mild cognitive impairment; NPD, non Parkinson's disease; PaS, parasubiculum; PD, Parkinson's disease; PDD, Parkinson's disease with dementia; PDMCI, Parkinson's disease with mild cognitive impairment; PrS, presubiculum; (r), right; S, subiculum.

Supplementary References

- Aarsland ARD. 2006. Management of Parkinson ' s Practical Considerations. *Drugs & Aging* 23: 807-22
- Apostolova LG, Beyer M, Green AE, Hwang KS, Morra JH, et al. 2010. Hippocampal, caudate, and ventricular changes in Parkinson's disease with and without dementia. *Movement Disorders* 25: 687-95
- Armstrong RA, Kotzbauer PT, Perlmuter JS, Campbell MC, Hurth KM, et al. 2014. A quantitative study of α -synuclein pathology in fifteen cases of dementia associated with Parkinson disease. *Journal of Neural Transmission* 121: 171-81
- Aybek S, Lazeyras F, Gronchi-Perrin A, Burkhard PR, Villemure JG, Vingerhoets FJG. 2009. Hippocampal atrophy predicts conversion to dementia after STN-DBS in Parkinson's disease. *Parkinsonism and Related Disorders* 15: 521-24
- Bouchard TP, Malykhin N, Martin WRW, Hanstock CC, Emery DJ, et al. 2008. Age and dementia-associated atrophy predominates in the hippocampal head and amygdala in Parkinson's disease. *Neurobiology of Aging* 29: 1027-39
- Braak H, Del Tredici K, Rüb U, De Vos RAI, Jansen Steur ENH, Braak E. 2003. Staging of brain pathology related to sporadic Parkinson's disease. *Neurobiology of Aging* 24: 197-211
- Brück A, Kurki T, Kaasinen V, Vahlberg T, Rinne JO. 2004. Hippocampal and prefrontal atrophy in patients with early non-demented Parkinson's disease is related to cognitive impairment. *Journal of Neurology, Neurosurgery and Psychiatry* 75: 1467-69

- Burton EJ, McKeith IG, Burn DJ, Williams ED, O'Brien JT. 2004. Cerebral atrophy in Parkinson's disease with and without dementia: A comparison with Alzheimer's disease, dementia with Lewy bodies and controls. *Brain* 127: 791-800
- Camicioli R, Moore MM, Kinney A, Corbridge E, Glassberg K, Kaye JA. 2003. Parkinson's disease is associated with hippocampal atrophy. pp. 784-90: *Mov Disord*
- Carlesimo GA, Piras F, Assogna F, Pontieri FE, Caltagirone C, Spalletta G. 2012. Hippocampal abnormalities and memory deficits in Parkinson disease: A multimodal imaging study. *Neurology* 78: 1939-45
- Chen B, Fan GG, Liu H, Wang S. 2015. Changes in anatomical and functional connectivity of Parkinson's disease patients according to cognitive status. *European Journal of Radiology* 84: 1318-24
- Chung SJ, Shin JH, Cho KH, Lee Y, Sohn YH, et al. 2017. Subcortical shape analysis of progressive mild cognitive impairment in Parkinson's disease. *Movement Disorders* 32: 1447-56
- Churchyard A, Lees AJ. 1997. The relationship between dementia and direct involvement of the hippocampus and amygdala in Parkinson's disease. *Neurology* 49: 1570-76
- Cohn M, Giannoylis I, De Belder M, Saint-Cyr JA, McAndrews MP. 2016. Associative reinstatement memory measures hippocampal function in Parkinson's Disease. *Neuropsychologia* 90: 25-32
- Cwc T, Ej B, Ig M, Dj B, Jt OB. 2005. Temporal lobe atrophy on MRI in Parkinson disease with dementia: a comparison with Alzheimer disease and dementia with Lewy bodies. *Neurology* 64: 861-65 5p

- Dickson DW, Schmidt ML, Lee VMY, Zhao ML, Yen SH, Trojanowski JQ. 1994. Immunoreactivity profile of hippocampal CA2/3 neurites in diffuse Lewy body disease. *Acta Neuropathologica* 87: 269-76
- Flores-Cuadrado A, Ubeda-Bañon I, Saiz-Sánchez D, de la Rosa-Prieto C, Martínez-Marcos A. 2016. Hippocampal α -synuclein and interneurons in Parkinson's disease: Data from human and mouse models. *Movement Disorders* 31: 979-88
- Foo H, Mak E, Chander RJ, Ng A, Au WL, et al. 2016. Associations of hippocampal subfields in the progression of cognitive decline related to Parkinson's disease. *NeuroImage: Clinical* 14: 37-42
- Gee M, Dukart J, Draganski B, Wayne Martin WR, Emery D, Camicioli R. 2017. Regional volumetric change in Parkinson's disease with cognitive decline. *Journal of the Neurological Sciences* 373: 88-94
- Goldman JG, Stebbins GT, Bernard B, Stoub TR, Goetz CG, deToledo-Morrell L. 2012. Entorhinal cortex atrophy differentiates Parkinson's disease patients with and without dementia. *Movement Disorders* 27: 727-34
- Harding AJ, Halliday GM. 2001. Cortical Lewy body pathology in the diagnosis of dementia. *Acta Neuropathologica* 102: 355-63
- Jokinen P, Brück A, Aalto S, Forsback S, Parkkola R, Rinne JO. 2009. Impaired cognitive performance in Parkinson's disease is related to caudate dopaminergic hypofunction and hippocampal atrophy. *Parkinsonism and Related Disorders* 15: 88-93
- Jokinen P, Scheinin N, Aalto S, Någren K, Savisto N, et al. 2010. [11C]PIB-, [18F]FDG-PET and MRI imaging in patients with Parkinson's disease with and without dementia. *Parkinsonism and Related Disorders* 16: 666-70

Junqué C, Ramírez-Ruiz B, Tolosa E, Summerfield C, Martí MJ, et al. 2005. Amygdalar and hippocampal MRI volumetric reductions in Parkinson's disease with dementia.

Movement Disorders 20: 540-44

Kamps S, Heuvel OAHD, Werf YDWD, Berendse HW, Weintraub D. 2018. Smaller subcortical volume in Parkinson patients with rapid eye movement sleep behavior disorder. Brain Imaging and Behavior i

Kandiah N, Zainal NH, Narasimhalu K, Chander RJ, Ng A, et al. 2014. Hippocampal volume and white matter disease in the prediction of dementia in Parkinson's disease.

Parkinsonism and Related Disorders 20: 1203-08

Kim HBA, Gearing M, Mirra SS. 1995. Ubiquitin-positive ca2/3 neurites in hippocampus coexist with cortical Lewy bodies. Neurology 45: 1768-70

Kunst J, Marecek R, Klobusickova P, Balazova Z, Anderkova L, et al. 2019. Patterns of Grey Matter Atrophy at Different Stages of Parkinson's and Alzheimer's Diseases and Relation to Cognition. Brain Topography 32: 142-60

Laakso MP, Partanen K, Riekkinen P, Lehtovirta M, Helkala EL, et al. 1996. Hippocampal volumes in Alzheimer's disease, Parkinson's disease with and without dementia, and in vascular dementia: An MRI study. Neurology 46: 678-81

Lee HM, Kwon KY, Kim MJ, Jang JW, Suh Si, et al. 2014. Subcortical grey matter changes in untreated, early stage Parkinson's disease without dementia. Parkinsonism and Related Disorders 20: 622-26

Lee SH, Kim SS, Tae WS, Lee SY, Lee KU, Jhoo J. 2013. Brain volumetry in Parkinson's disease with and without dementia: Where are the differences? Acta Radiologica 54: 581-

- Lenka A, Ingalhalikar M, Shah A, Saini J, Arumugham SS, et al. 2018. Hippocampal subfield atrophy in patients with Parkinson's disease and psychosis. *Journal of Neural Transmission* 125: 1361-72
- Low A, Foo H, Yong TT, Tan LCS, Kandiah N. 2019. Hippocampal subfield atrophy of CA1 and subiculum structures predict progression to dementia in idiopathic Parkinson's disease. *Journal of Neurology, Neurosurgery and Psychiatry* 90: 681-87
- Mattila PM, Rinne JO, Helenius H, Röyttä M. 1999. Neuritic degeneration in the hippocampus and amygdala in Parkinson's disease in relation to Alzheimer pathology. *Acta Neuropathologica* 98: 157-64
- Melzer TR, Watts R, MacAskill MR, Pitcher TL, Livingston L, et al. 2012. Grey matter atrophy in cognitively impaired Parkinson's disease. *Journal of Neurology, Neurosurgery and Psychiatry* 83: 188-94
- Messina D, Cerasa A, Condino F, Arabia G, Novellino F, et al. 2011. Patterns of brain atrophy in Parkinson's disease, progressive supranuclear palsy and multiple system atrophy. *Parkinsonism and Related Disorders* 17: 172-76
- Mihaescu AS, Masellis M, Graff-Guerrero A, Kim J, Criaud M, et al. 2019. Brain degeneration in Parkinson's disease patients with cognitive decline: a coordinate-based meta-analysis. *Brain Imaging and Behavior* 13: 1021-34
- Nagano-Saito A, Washimi Y, Arahata Y, Kachi T, Lerch JP, et al. 2005. Cerebral atrophy and its relation to cognitive impairment in Parkinson disease. *Neurology* 64: 224-29
- Noh SW, Han YH, Mun CW, Chung EJ, Kim EG, et al. 2014. Analysis among cognitive profiles and gray matter volume in newly diagnosed Parkinson's disease with mild cognitive impairment. *Journal of the Neurological Sciences* 347: 210-13

- Novellino F, Vasta R, Sarica A, Chiriaco C, Salsone M, et al. 2018. Relationship between Hippocampal Subfields and Category Cued Recall in AD and PDD: A Multimodal MRI Study. *Neuroscience* 371: 506-17
- Nyberg EM, Tanabe J, Honce JM, Krmpotich T, Shelton E, et al. 2015. Morphologic changes in the mesolimbic pathway in Parkinson's disease motor subtypes. *Parkinsonism and Related Disorders* 21: 536-40
- Pereira JB, Junqué C, Bartrés-Faz D, Ramírez-Ruiz B, Martí M-J, Tolosa E. 2013. Regional vulnerability of hippocampal subfields and memory deficits in Parkinson's disease. *Hippocampus* 23: 720-28
- Radziunas A, Deltuva VP, Tamasauskas A, Gleizniene R, Pranckeviciene A, et al. 2018. Brain MRI morphometric analysis in Parkinson's disease patients with sleep disturbances. *BMC Neurology* 18
- Rektorova I, Biundo R, Marecek R, Weis L, Aarsland D, Antonini A. 2014. Grey matter changes in cognitively impaired Parkinson's disease patients. *PLoS ONE* 9
- Schneider CB, Donix M, Linse K, Werner A, Fauser M, et al. 2017. Accelerated age-dependent hippocampal volume loss in Parkinson disease with mild cognitive impairment. *American Journal of Alzheimer's Disease and other Dementias* 32: 313-19
- Summerfield C, Junqué C, Tolosa E, Salgado-Pineda P, Gómez-Ansón B, et al. 2005. Structural Brain Changes in Parkinson Disease With Dementia. *Archives of Neurology* 62: 281-81
- Vasconcellos LF, Pereira JS, Adachi M, Greca D, Cruz M, et al. 2018. Volumetric brain analysis as a predictor of a worse cognitive outcome in Parkinson's disease. *Journal of Psychiatric Research* 102: 254-60

- Wang N, Zhang L, Yang HG, Luo XG, Fan GG. 2019. Do multiple system atrophy and Parkinson's disease show distinct patterns of volumetric alterations across hippocampal subfields? An exploratory study. European Radiology 29: 4948-56
- Yao N, Cheung C, Pang S, Shek-kwan Chang R, Lau KK, et al. 2016. Multimodal MRI of the hippocampus in Parkinson's disease with visual hallucinations. Brain Structure and Function 221: 287-300
- Zeng Q, Guan X, Law Yan Lun JCF, Shen Z, Guo T, et al. 2017. Longitudinal Alterations of Local Spontaneous Brain Activity in Parkinson's Disease. Neuroscience Bulletin 33: 501-09
- Zhang Y, Zhang J, Xu J, Wu X, Zhang Y, et al. 2014. Cortical gyration reductions and subcortical atrophy in Parkinson's disease. Movement Disorders 29: 122-26